Development 133, 275-285 doi:10.1242/dev.02191

Use of time-lapse imaging and dominant negative receptors to dissect the steroid receptor control of neuronal remodeling in *Drosophila*

Heather L. D. Brown[1,*], Lucy Cherbas[2], Peter Cherbas[2] and James W. Truman[1]

During metamorphosis, the reorganization of the nervous system of *Drosophila melanogaster* proceeds in part through remodeling of larval neurons. In this study, we used in-vitro imaging techniques and immunocytochemistry to track the remodeling of the thoracic ventral neurosecretory cells. Axons of these neurons prune their larval arbors early in metamorphosis and a larger, more extensive adult arbor is established via branch outgrowth. Expression of EcR dominant negative constructs and an EcR inverted repeat construct resulted in pruning defects of larval axon arbors and a lack of filopodia during pruning, but showed variable effects on outgrowth depending on the construct expressed. Cells expressing either UAS-EcR-B1^{W650A} or UAS-EcR-A^{W650A} lacked filopodia during the outgrowth period and formed a poorly branched, larval-like arbor in the adult. Cells expressing UAS-EcR-B1^{F645A}, UAS-EcR-B2^{W650A} or UAS-IR-EcR (core) showed moderate filopodial activity and normal, albeit reduced, adult-like branching during outgrowth. These results are consistent with the role of activation versus derepression via EcR for successive phases of neuronal remodeling and suggest that functional ecdysone receptor is necessary for some, but not all, remodeling events.

KEY WORDS: *Drosophila*, Axon remodeling, Ecdysone receptor, Metamorphosis

INTRODUCTION

Steroid hormones control the body plan changes of holometabolous insects during metamorphosis. Ecdysone and its metabolite 20-Hydroxyecdysone (20E) drive the remodeling of the larval body during this period, including the rewiring of the nervous system for adult function (Weeks and Truman, 1985). This rewiring proceeds through programmed cell death of larval neurons, maturation of adult-specific neurons, and remodeling of persistent larval neurons for adult use (Tissot and Stocker, 2000; Truman, 2005; Weeks, 1999). These persistent neurons prune back their axonal and dendritic branches early in metamorphosis and then grow new, adult-specific arbors, establishing the neuronal circuitry necessary for the adult. The ecdysteroids, particularly 20E, act through their receptor to mediate pruning and outgrowth in the nervous system of *Drosophila melanogaster*. The ecdysone receptor is an obligate heterodimer formed from two nuclear receptors: EcR and the RXR-ortholog Ultraspiracle (USP) (Koelle et al., 1991; Yao et al., 1992). The EcR-USP heterodimer binds to specific ecdysone response elements (EcRE) in DNA to regulate transcription of target genes (Cherbas et al., 1991).

The EcR/USP complex, referred to in this paper as the ecdysone receptor, is able to both activate and repress target genes, depending on the presence or absence of ecdysteroids (reviewed by Kozlova and Thummel, 2000). When ecdysteroid is absent and sufficient amounts of a co-repressor such as SMRTER are present, the ecdysone receptor is able to repress transcription (Dressel et al., 1999; Tsai et al., 1999). When ecdysteroid is present, it binds to the ecdysone receptor complex, causing a conformational change that promotes the release of co-repressors and the binding of co-activators, initiating transcription of early response genes (Bai et al., 2000; Sedkov et al., 2003). Both the activational and repressive actions of the receptor are functionally significant in vivo. For example, USP null clones in the wing disc show a failure to express some ecdysone target genes, while others are expressed prematurely, and the clones show precocious differentiation of sensory neurons (Schubiger and Truman, 2000). This mixed response suggests that although the steroid acts via the EcR/USP complex, in some cases it is through activation while in others it is through derepression.

EcR is a member of the nuclear receptor superfamily. Its N-terminus is composed of a variable A/B domain, and may contain a ligand-independent activational region (AF1). The E domain contains the main dimerization domain and another activational region (AF2) contingent on ligand-binding (Robinson-Rechavi et al., 2003). There are three EcR isoforms in *D. melanogaster:* EcR-A, EcR-B1 and EcR-B2. Studies have shown that EcR-B1 and EcR-B2 both have strong activation functions in their A/B regions, while EcR-A may have an inhibitory function (Hu et al., 2003; Mouillet et al., 2001). All three EcR isoforms bind equally well to the DNA EcRE (Cherbas et al., 1991; Mouillet et al., 2001) and to ecdysteroid (Dela Cruz et al., 2000), but they have different spatial and temporal expressions and induce different cellular responses (Cherbas et al., 2003; Talbot et al., 1993; Truman et al., 1994).

Variable cellular responses to the three EcR isoforms are particularly evident in the remodeling nervous system. High levels of EcR-B1 early in metamorphosis have been associated with pruning of larval branches (Truman et al., 1994). In many remodeling neurons, EcR-B1 expression decreases and EcR-A expression becomes prominent as the neuron begins its adult outgrowth. By contrast to remodeling larval neurons, arrested imaginal neurons born during larval life express only EcR-A at the start of metamorphosis as they begin their adult outgrowth (Truman et al., 1994). Experiments examining pruning in both thoracic ventral (Tv) neuron dendrites (Schubiger et al., 1998) and mushroom body axons (Lee et al., 2000) showed that EcR-B mutants lose their ability to prune, and can be rescued by expression of either EcR-B1 or EcR-B2 but not

[1]Department of Biology, University of Washington, Seattle WA 98195, USA.
[2]Department of Biology and Center for Genomics and Bioinformatics, Indiana University, Bloomington, IN 47405, USA.

*Author for correspondence (e-mail: hdbrown@u.washington.edu)

Accepted 31 October 2005

EcR-A (Lee et al., 2000; Schubiger et al., 2003; Schubiger et al., 1998). EcR-B1-specific mutants prune normally, indicating either that B1 and B2 are functionally redundant or that B2 is the primary isoform driving pruning (Schubiger et al., 1998). These experiments suggest that the EcR-B isoforms are associated with pruning and reorganizational responses while EcR-A is responsible for outgrowth of arbors. However, the specific role each EcR isoform has in directing precise cellular responses during neuronal remodeling is still not understood.

In this study, we investigated the role of EcR in Tv cell axonal remodeling. Our results highlight the specific axonal events during Tv cell remodeling, allowing us to analyze in detail both pruning and outgrowth. Results from cell-autonomous expression of EcR dominant negative constructs and EcR RNAi show that, while activation is necessary for early pruning events, it may not be required for later remodeling events.

MATERIALS AND METHODS

Fly stocks

CMA-EcR-B1-d655-F645A, CMA-EcR-d655-W650A, and their P-element vector derivatives UAS-EcR-B1-d655-F645A (referred to in this paper as UAS-EcR-B1^{F645A}) and UAS-EcR-B1-d655-W650A (referred to in this paper as UAS-EcR-B1^{W650A}) were described by Hu et al. (Hu et al., 2003) and Cherbas et al. (Cherbas et al., 2003). Similar constructs based on the A and B2 isoforms of EcR, UAS-EcR-A^{F645A}, UAS-EcR-A^{W650A} and UAS-EcR-B2^{W650A} were made as follows: the 5′ portion of the EcR-B1 coding sequence was excised from a mutant CMA-EcR-B1 plasmid with *Bam*HI (which cuts upstream of the start of translation) and *Asc*I (which cuts within the coding sequence for the common-region DNA-binding domain), and replaced with the corresponding *Bam*HI-*Asc*I fragment from either CMA-EcR-A or CMA-EcR-B2 (Hu et al., 2003) to generate a coding sequence containing the A or B2 isoform-specific N-terminus and the dominant negative mutation (F645A or W650A). The entire coding region for the mutant EcR was then excised with *Bam*HI and *Nhe*I and inserted between the *Bgl*II and *Xba*I sites of the vector pUAST, to generate the responder transposon. UAS-EcR-B1^{F645A}, UAS-EcR-B1^{W650A}, UAS-EcR-B2^{W650A} and UAS-EcR-A^{W650A} were inserted into flies via P-element transformation to create homozygous fly stocks (Cherbas et al., 2003). EcR RNAi was performed using the CA104 stock containing an inserted EcR core inverted repeat construct (UAS-IR-EcR) from C. Antoniewski (Schubiger et al., 2005). To facilitate cell-autonomous expression of these constructs in the Tv cells, the above stocks were crossed with a fly stock containing both the GAL4 driver (Brand and Perrimon, 1993) under control of the FMRF-amide promoter and a UAS-GFP insert (Lee and Luo, 1999) that targets CD8::GFP to the membrane. The ywUASmCD8::GFP; FG10 stock made use of a FMRF-amide promoter construct created by S. Robinow, University of Hawaii (Schubiger et al., 2003; Suster et al., 2003). Progeny expressed both membrane-bound GFP and either EcR dominant negative construct or IR-EcR (core) cell autonomously in the Tv neurosecretory cells.

Immunocytochemistry

Central nervous systems were dissected and fixed for 20-30 minutes in 4% paraformaldehyde, followed by multiple rinses with PBS containing 1% Triton X-100 (PBS-Tx). Tissue was blocked with 5% normal donkey serum for 15 minutes followed by transfer to a solution of primary antibodies and incubation overnight. Primary antibodies used were monoclonal mouse anti-SCP (Masinovsky et al., 1988), rat anti-mCD8 (1:200, CALTAG) and mouse anti-EcR (IID9.6, common) (Talbot et al., 1993). After several rinses with PBS-Tx, the tissues were incubated overnight in secondary antibody (1:200 in PBS-Tx of Texas red conjugated donkey anti-mouse IgG, Texas red conjugated donkey anti-rabbit IgG, or FITC conjugated donkey anti-rat IgG; Jackson ImmunoResearch). Nervous systems were rinsed several times in PBS and attached to polylysine-coated coverslips, then dehydrated, cleared in xylene and mounted in DPX (Fluka). For quantification of EcR or mCD8 immunoreactivity, all genotypes to be compared were dissected, antibody stained and imaged as one batch.

Staging and imaging

Animals were collected at white puparia and maintained at either 25°C or 29°C. Late wandering larvae were distinguished by their enlarged salivary glands. For live imaging, whole intact nervous systems were dissected from staged animals, leaving the ring gland intact. Tissue was attached to a polylysine-coated coverslip and inverted onto a metal imaging chamber (Kiehart et al., 1994). This chamber was bounded on the bottom by an oxygen-permeable membrane (model 5793, YSI, Yellow Springs, OH) and filled with Shields and Sang M3 insect culture media (Sigma, St Louis, MO) with 7.5% fetal bovine serum (Sigma). For live imaging, a Bio-Rad Radiance 2000 confocal microscope equipped with a 488 nm Kr/Ar laser was used. Individual *Z*-stacks with a step size of 1.05 μm were taken every 20 minutes over a 3-18-hour period. The development of explanted nervous systems slowed in culture, and 2 hours of time in vitro was roughly equivalent to 1 hour in vivo (Gibbs and Truman, 1998). The age of *Z*-stack projections from time-lapse video was calculated by referring to the time of explantation. Time-lapse movies were created from the *Z*-stacks using NIH ImageJ (http://rsb.info.nih.gov/ij/).

Analysis

Arbor area, arbor footprint, filopodial quantification and quantification of EcR and mCD8 immunoreactivity were calculated using NIH ImageJ. For arbor area, all images were adjusted to a similar threshold, converted to black and white, and quantified by counting the number of pixels. To obtain the arbor footprint, a polygon was created by connecting the outer edges of the axon arbor with straight lines; then the total number of pixels in the area inside the polygon were counted. Filopodia were quantified by manual counting at each hour for each neuromere. For more developed arbors that were already fasciculated, all filopodia were counted and divided by three to get a filopodia count for each neuromere. To quantify relative EcR and mCD8 immunoreactivity, fixed cell bodies were imaged from each genotype. Each nucleus was selected and the mean intensity determined using ImageJ. The mean intensity for the background area was subtracted from the selected area to get the net mean intensity for each nucleus. As all animals used had one copy of mCD8::GFP, the immunoreactivity of mCD8 should be similar among all genotypes. The ratio of EcR to mCD8 immunoreactivity was calculated by dividing the net mean EcR intensity by the net mean mCD8 intensity. To calculate statistical significance, a non-paired *t*-test (α=0.05) was run using SigmaStat and SPSS software.

RESULTS

Remodeling of the Tv neuron axon arbors

The Tv neurons are paired neurosecretory cells located in each of the thoracic neuromeres. During larval life, the axons of each segmental pair of Tv cells wrap around two support cells in a compact, globular structure, forming a neurohemal organ (Nassel et al., 1988). The neurohemal organs project above the dorsal surface of the central nervous system (CNS), while the somata and dendrites of the Tv cells reside within the neuromere (Fig. 1A). Although the central dendrites of these cells had severely pruned back by 5-6 hours after puparium formation (apf) (Schubiger et al., 1998), the start of axonal remodeling did not begin until approximately 10 hours apf, with the larval arbor being completely pruned by 18 hours apf. Outgrowth of adult branches began between 18 and 20 hours apf, and was essentially finished by 48 hours apf, forming a complex mesh-like arbor spreading out over the dorsal surface of the CNS (Fig. 1C). The branching of the arbor changed little between 48 hours and adult eclosion (approximately 96 hours apf).

We used confocal live imaging to visualize axon pruning and growth in short-term explanted *Drosophila* nervous systems. The Tv cells were vitally labeled using the FG10-GAL4 driver to express the membrane marker CD8::GFP in these cells (Fig. 1B). The superficial location of the Tv cell axons on the dorsal surface of the explanted CNS aided live imaging. At pupariation, the neurohemal sites appeared much the same as in the larva and we observed no

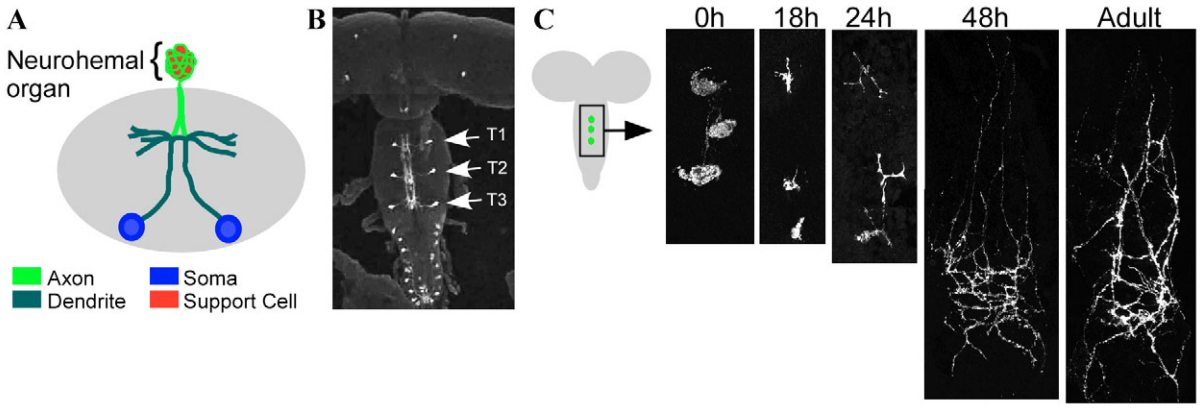

Fig. 1. Metamorphosis of the thoracic ventral (Tv) neurosecretory cells. (**A**) Schematic transverse section of the ventral nervous system, showing the axons, dendrites and cell bodies of a pair of Tv cells, before metamorphosis. The axons are wrapped around a pair of support cells (dorsal neurohemal organ), situated outside the neural sheath. (**B**) Projected confocal *Z*-stack of CD8::GFP expression in the thoracic neuromeres of an early metamorphic individual (18 hours apf) of the genotype UAS-CD8::GFP;FG10-GAL4. Expression in the thorax is limited to the three pairs of Tv neurons (arrows point to somata). (**C**) Dorsal view of the Tv cell axons, immunostained with α-SCP, at various time points during metamorphosis.

morphological changes from late third instar through 3 to 5 hours apf. Beginning around 5 hours apf, however, fine filopodia started sprouting from the axon arbor (Fig. 2A), and approximately 5-7 hours later the neurons began pruning back their axonal arbor. During pruning, we saw active filopodia both on the regressing larval portion of the arbor and in an adult growth zone that was forming beneath the neurohemal organ (Fig. 2B). Most filopodia present on the neurohemal organ and the growth zone changed considerably in length during each 20-minute interval, either extending, shortening or branching. In instances in which we could follow the regression of individual axon branches, we saw only retraction and no sign of branch fragmentation (local degeneration) as described for mushroom body axons (Watts et al., 2003) and dendrites of the dendritic arborizing neurons (Williams and Truman, 2005). Addition of hemolymph to the culture, supplying a source of hemocytes, did not affect pruning, and no severing of branches occurred (data not

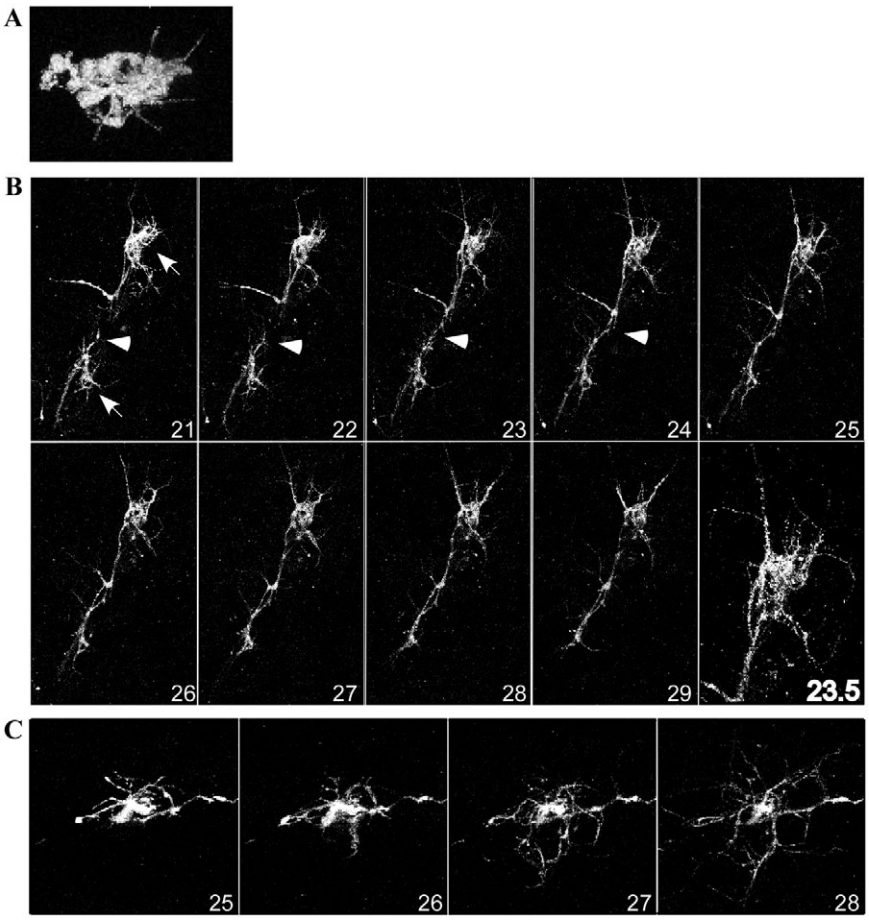

Fig. 2. *Z*-stack projections from live imaging time-lapse videos, showing changes in the axonal arbors of Tv neurons. (**A**) Enlarged still of the most anterior axon arbor (T1) at 6.5 hours apf, showing filopodia extending from the neurohemal organ. (**B**) *Z*-stack time-lapse projection of the T2 (bottom) and T3 (top) neurohemal organs (arrows) from 21 to 29 hours apf, every 60 minutes. Pruning can be seen clearly as T2 decreases in size from 21 to 29 hours apf. Filopodia from the growth zone under each neurohemal organ fasciculate (arrowheads). The last panel is an enlarged still of the T3 neurohemal organ at 23.5 hours apf, showing the large number of filopodia. (**C**) *Z*-stack time-lapse projection of a pruned T3 axon arbor from 25 to 28 hours apf, showing the dramatic outgrowth that occurs between 25 and 28 hours apf.

shown). Filopodia in the growth zone area continued to be active as the larval axonal arbor disappeared, and eventually stabilized to form branches at the base of the pruned neurohemal organ (Fig. 2B-C). We observed filopodia on both the shaft and tip of primary branches as they extended to form a mesh-like network of axonal branches. Filopodia persisted as late as 56 hours apf, as the arbor continued to expand through activity on the outermost branches of the network (not shown).

Effects of dominant negative EcR isoforms on axonal pruning

As the ecdysone receptor is key in directing neuronal remodeling, cell-autonomous expression of dominant negative EcR (EcR-DN) should poison the cell response to ecdysteroid and disrupt pruning of Tv cell axons. Two types of EcR-DN constructs were used, both containing a point mutation in helix 12 of the ligand-binding domain (Cherbas et al., 2003). The F645A mutation is in the co-activator binding groove in the AF2 domain and results in a receptor that binds ligand but cannot mediate activation. The W650A mutation prevents steroid binding and, consequently, also results in a lack of ligand-dependent activation. In vitro, these EcR-DNs bind DNA and USP normally, and act as competitive inhibitors of endogenous wild-type EcR (Cherbas et al., 2003). As both types of EcR-DNs are equally effective at suppressing ligand-dependent activation, differences between the biological effects of the two are probably due to the fact that one can bind steroid and the other cannot. The latter ability is significant, because the unliganded EcR/USP complex can act as a repressor. Both the F645A and W650A-based EcR-DNs are capable of mediating this repression (Hu et al., 2003), but their differences in ligand binding may mean that one is a conditional repressor whereas the other is a constitutive repressor (see Discussion).

We compared the effects of the F645A or W650A substitution in EcR-B1 and the W650A substitution in all three isoforms (EcR-B1, EcR-B2 and EcR-A). Because endogenous EcR shows no isoform specificity in binding to DNA (Mouillet et al., 2001), we assumed that expressing EcR dominant negative at high levels in the cell displaced the endogenous EcR in a non-isoform-specific manner. The different A/B regions of the EcR-DNs should have little effect on the activation capacities of the modified receptor, because the AF2-mediated activation functions are blocked in all of them. However, since the EcR-DNs retain their repressor function, the use of isoform-specific W650A-based EcR-DNs allowed us to probe the role of the A/B region of the isoforms in processes that might be mediated via derepression. Comparison of the F645A mutation to the W650A mutation in EcR-B1 let us analyze the need for activation over derepression of the AF2 domain.

Cells expressing the individual EcR-DN constructs showed similar pruning responses, regardless of which construct was present. Fig. 3 shows the progression of pruning for neurons expressing each of the EcR-DN constructs. All cells expressing the EcR-DN were of normal size and larval morphology at the start of metamorphosis. By 18 hours apf, however, the cells expressing EcR-DN showed only modest pruning compared with control cells (expressing GFP only), and by 24 hours apf they still had a reduced larval neurohemal organ with no sign of branch outgrowth. Neurons expressing CD8::GFP only (control cells), by contrast, had completely pruned their neurohemal organs and were beginning branch outgrowth by this time (Fig. 3). Live imaging through this pruning period also gave similar results for all EcR-DN constructs. Notably, neurons expressing any EcR-DN construct lacked filopodia before and during the pruning time period (Fig. 4A). As with the immunocytochemistry, live imaging revealed slow and incomplete pruning of the larval neurohemal organ. These larval arbors were retained well past the time of pruning into the period when the cell should switch to outgrowth (Fig. 4B-C).

Effects of dominant-negative EcR isoforms on axon outgrowth

Although expression of the various EcR-DN constructs resulted in similar effects during the pruning phase, they were quite different in how they affected outgrowth. Neurons expressing EcR-B1^{F645A} or EcR-B2^{W650A} showed relatively mild effects on adult outgrowth characteristics, whereas neurons expressing EcR-A^{W650A} or EcR-B1^{W650A} were much more severely affected. At both 48 hours apf and in the adult, the neurons expressing EcR-B1^{F645A} or EcR-

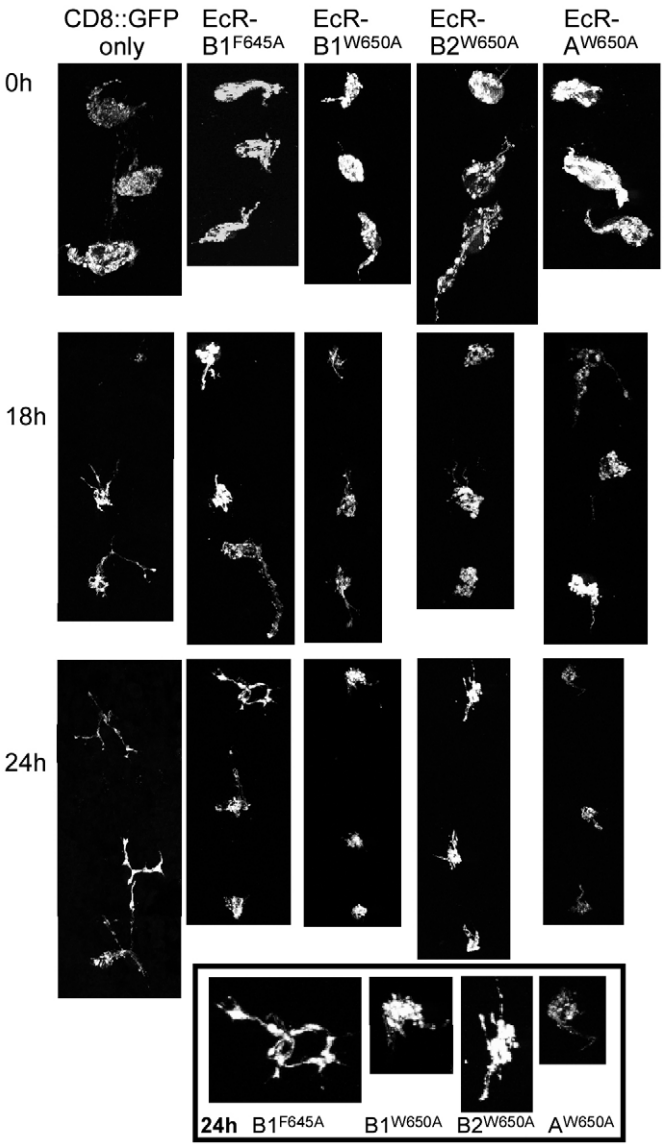

Fig. 3. Immunocytochemistry (α-SCP) of Tv cell axon arbors during the pruning phase of remodeling, for control cells and cells expressing EcR-DN. Variability in nervous system size and spacing of Tv cell neurohemal organs was seen in all treatments and did not appear to be correlated with any particular treatment. Inset: magnification of the T1 axon arbor at 24 hours apf of cells expressing EcR-DNs.

B2^{W650A} had a moderately elaborated, branched arbor that formed a loose reticulum at the junction of the T2 and T3 neuromeres and had two to four branches that extended anteriorly, often into the neck connectives. Unlike in control animals, cells expressing these EcR-DNs often had a clumped tangle of branches in the center of the adult arbor (Fig. 5A). Neurons that expressed EcR-A^{W650A} had a clumped arbor at 48 hours apf, reminiscent of the larval arbor, but also showed a few adult-like fasciculating branches. Arbors of cells expressing EcR-B1^{W650A} were the most severely affected, with prominent larval-like neurohemal organs and occasional branches that extended over the surface of the CNS. These branches only rarely showed higher order branching. Measurements of the area covered by the new arbor under the various conditions show that none of the EcR-DNs made an arbor as extensive as seen in controls, but the most reduced arbors were seen in cells expressing EcR-A^{W650A} or EcR-B1^{W650A} (Fig. 5B).

Live imaging data emphasized the differences seen between the outgrowth patterns of cells expressing EcR-B1^{F645A} or EcR-B2^{W650A} versus the other EcR-DN constructs. Although cells expressing the EcR-DNs showed no filopodia during the pruning phase, those expressing EcR-B1^{F645A} or EcR-B2^{W650A} started extending filopodia after 24 hours apf (Fig. 6). Filopodia formed on both the remnant of the neurohemal organ and below it, in the growth zone. Filopodia in both locations stabilized into branches that fasciculated to form an arbor with both adult and larval characteristics. As filopodia located on the neurohemal organ extended and stabilized into branches, the remnant neurohemal organ partially fragmented, resulting in an adult-like arbor with clumped varicosities and a dense center. Fig. 4B shows filopodia emanating from the remaining larval arbor of cells expressing EcR-B1^{F645A}. Although cells expressing EcR-B1^{F645A} and EcR-B2^{W650A} formed branches during this outgrowth phase, these axon arbors differed in appearance from branches on

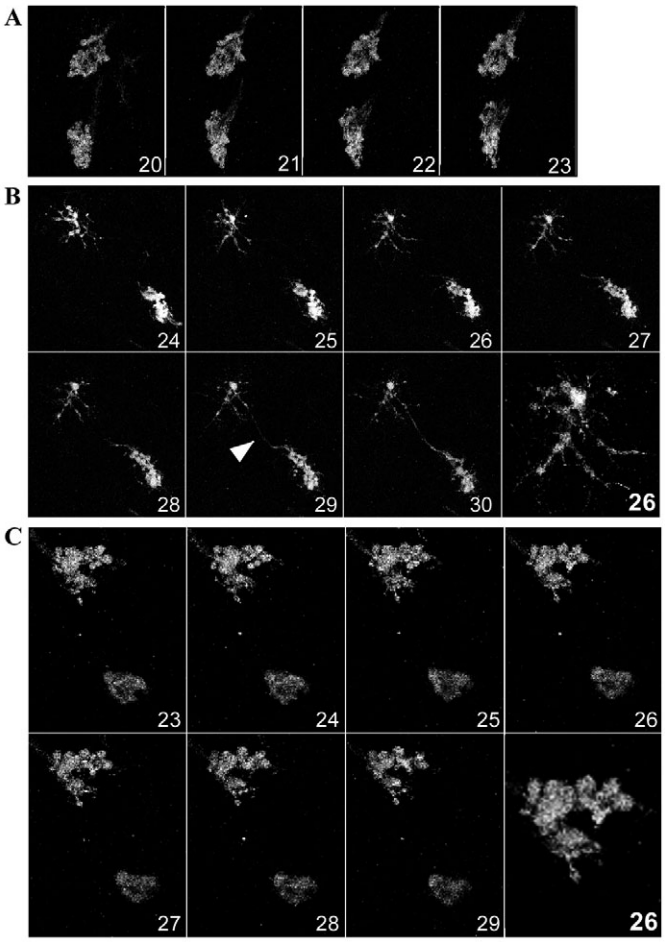

Fig. 4. *Z*-stack projections from time-lapse videos of axons from Tv cells expressing EcR-B1^{F645A} or EcR-B1^{W650A}. (**A**) *Z*-stack time-lapse projection of two neurohemal organs (T2 above, T3 below) from cells expressing EcR-B1^{F645A} from 20 to 23 hours apf, 60 minutes apart. No filopodia are visible during this time period. (**B**) *Z*-stack projections of remodeling axon arbors from cells expressing EcR-B1^{F645A}. From 24 to 30 hours apf, filopodia from the partially pruned T1 (above) fasciculate and stabilize with filopodia from T2 (arrowhead). The last panel is an enlarged still of T1 at 26 hours apf, showing filopodia. (**C**) *Z*-stack time-lapse projections of axon arbors (T3 above, T2 below) from cells expressing EcR-B1^{W650A}, from 23 to 29 hours apf, with an enlarged still at 26 hours apf, showing no filopodia.

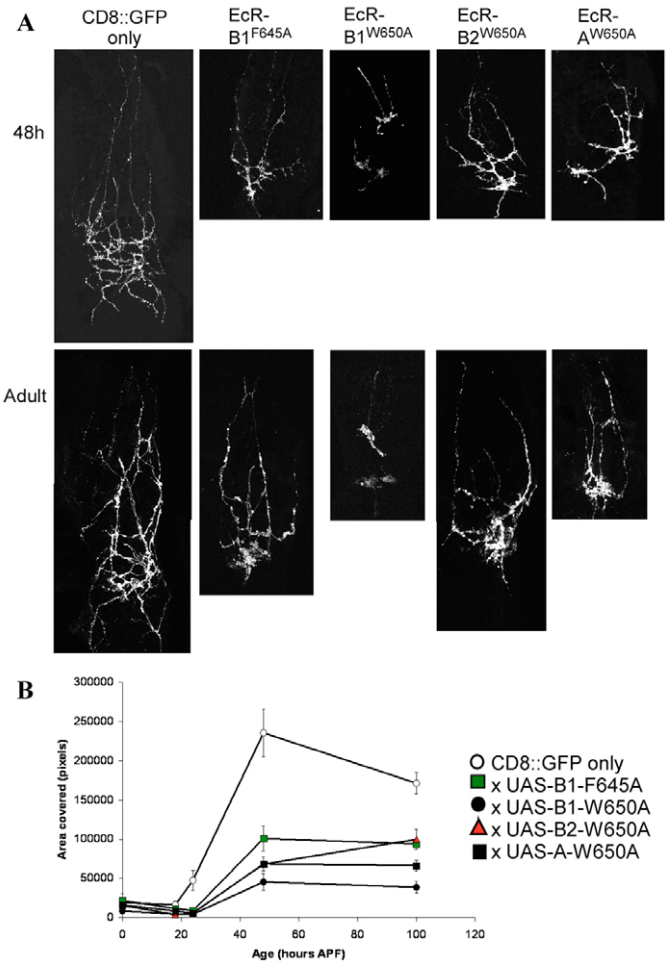

Fig. 5. Immunocytochemistry (α-SCP) of Tv cell axon arbors during the outgrowth phase of remodeling and quantification of arbor size during remodeling for control cells and cells expressing EcR-DN. (**A**) Immunocytochemistry (α-SCP) of Tv cell axon arbors during outgrowth, for control cells and cells expressing EcR-DN. (**B**) Comparison of arbor footprints from pupariation to adult. Arbor footprint was measured by taking a pixel count of the polygon created by connecting the outermost spread of the axon arbor.

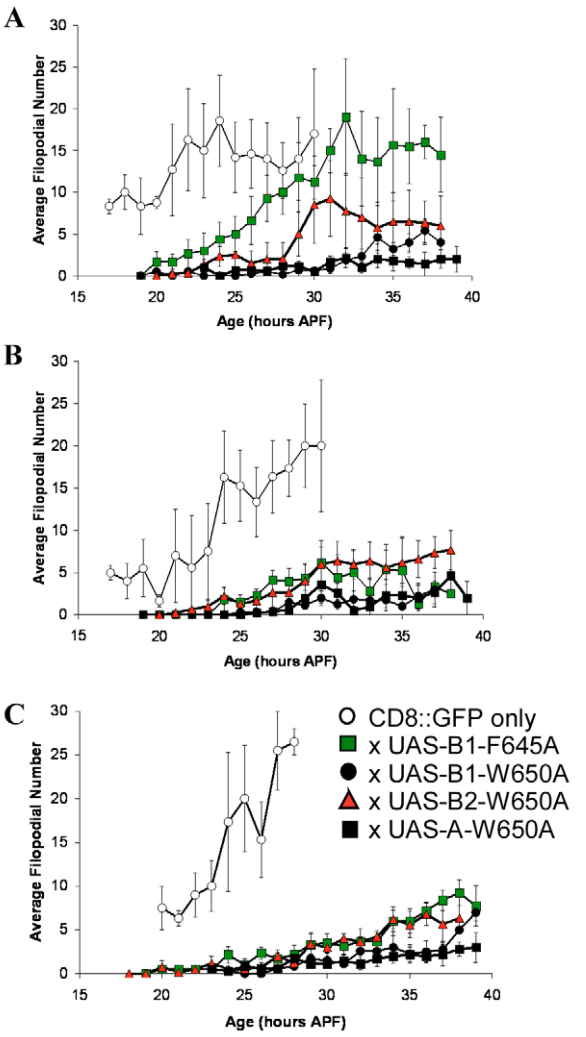

Fig. 6. Quantitative analysis of filopodial activity for Tv cell axons. Average filopodial number per hour for control cells and cells expressing EcR-DN was calculated from live imaging data for T1 (**A**), T2 (**B**) and T3 (**C**).

cells expressing CD8::GFP-only. Axons from cells expressing these two dominant negatives were blebbier, with swollen regions along the branches. Interestingly, the cells expressing EcR-B1^{F645A} and EcR-B2^{W650A} had fewer filopodia in the meso- and metathoracic neuromeres compared with their prothoracic counterparts (Fig. 6).

By contrast to the above EcR-DNs, cells expressing EcR-B1^{W650A} or EcR-A^{W650A} failed to extend filopodia during the outgrowth phase. The rare filopodial-like structures that we saw were very short, stubby and less active than those seen on control cells or cells expressing EcR-B1^{F645A} or EcR-B2^{W650A} (Fig. 4C). They did not change extensively in length or branching during each 20-minute interval, and once established they persisted without a significant length change for 60 minutes or more. The arbors of these cells remained very larval-like to the end of imaging and did not show the extended branches seen on the arbors of cells expressing EcR-B1^{F645A} or EcR-B2^{W650A}.

Effects of dominant negative EcR expression are qualitative

The differences seen during outgrowth of neurons expressing the various EcR-DNs could represent a qualitative difference reflecting the molecular action of EcR or a simple quantitative effect due to varying expression levels of the EcR-DN inserts. We addressed this issue in three different ways: expression of the same EcR-DN constructs from different insertion sites; comparison of neurons from animals raised at 25°C versus 29°C; and quantitative immunocytochemistry to determine the relative amounts of protein expressed in Tv cell bodies for all EcR-DN constructs.

We examined the arbors of cells expressing two different inserts of EcR-B2^{W650A} and of EcR-A^{W650A}. There was no significant difference seen between the arbor areas for the individual inserts of the same construct. This was also true for the arbor footprints; the cells expressing either of the EcR-B2^{W650A} inserts were similar, and cells expressing either of the EcR-A^{W650A} inserts were similar (Table 1).

As increasing temperature boosts the efficiency of GAL4-UAS expression, raising animals at 29°C leads to an increase in target protein production (Brand and Perrimon, 1993). Therefore, we compared the arbor areas and footprints of the adult axonal arbors for cells expressing the various EcR-DNs at 25°C versus 29°C. The only significant difference seen was between the arbor footprints of cells expressing the EcR-B1^{W650A} at the different temperatures. At 25°C, the footprint pixel count was 38,578 (n=8), while at 29°C it was reduced to 12,422 (n=10, P=0.01). The difference in the arbor area of cells expressing EcR-B1^{W650A} at 25°C versus 29°C was not significant, with pixel counts of 3306 and 3766, respectively (P=0.41). All of the other EcR-DNs were not significantly different for either arbor area or arbor footprint at the different temperatures (Table 1).

We also used quantitative immunocytochemistry to determine the relative protein levels in nuclei of cells expressing each individual EcR-DN. EcR levels were significantly higher in cells expressing EcR-DN than in control cells (P<0.05; Fig. 7A). Although EcR levels varied between the cells expressing different EcR-DNs, the differences in protein level did not correspond with the severity of axonal phenotype. Neurons expressing EcR-B1^{F645A} had a relatively higher EcR level than those expressing EcR-B1^{W650A}, but the cells expressing EcR-B1^{W650A} had a more severe phenotype. CD8 levels in all cells examined did not differ significantly; the ratio of EcR to

Table 1. Average pixel counts and s.e.m. for arbor area and arbor footprint measurements of cells expressing EcR-DN at 25°C and 29°C

	25°C			29°C		
Construct expressed	n	Arbor area ($\times 10^3$)	Arbor footprint ($\times 10^3$)	n	Arbor area ($\times 10^3$)	Arbor footprint ($\times 10^3$)
EcR-B1^{F645A}	11	6.1±0.5	93.9±7.0	7	7.0±0.8	71.5±10.3
EcR-B1^{W650A}	8	3.3±0.5	38.6±7.6	10	3.8±0.3	12.4±2.1
EcR-A^{W650A} TP5	16	5.5±0.5	66.4±6.7	7	4.1±0.6	44.2±6.0
EcR-A^{W650A} TP3	–	–	–	8	3.8±0.4	43.1±5.7
EcR-B2^{W650A} TP1	6	7.3±0.9	99.7±12.5	9	6.7±0.5	97.9±6.6
EcR-B2^{W650A} TP5	–	–	–	12	7.3±0.4	83.1±7.7

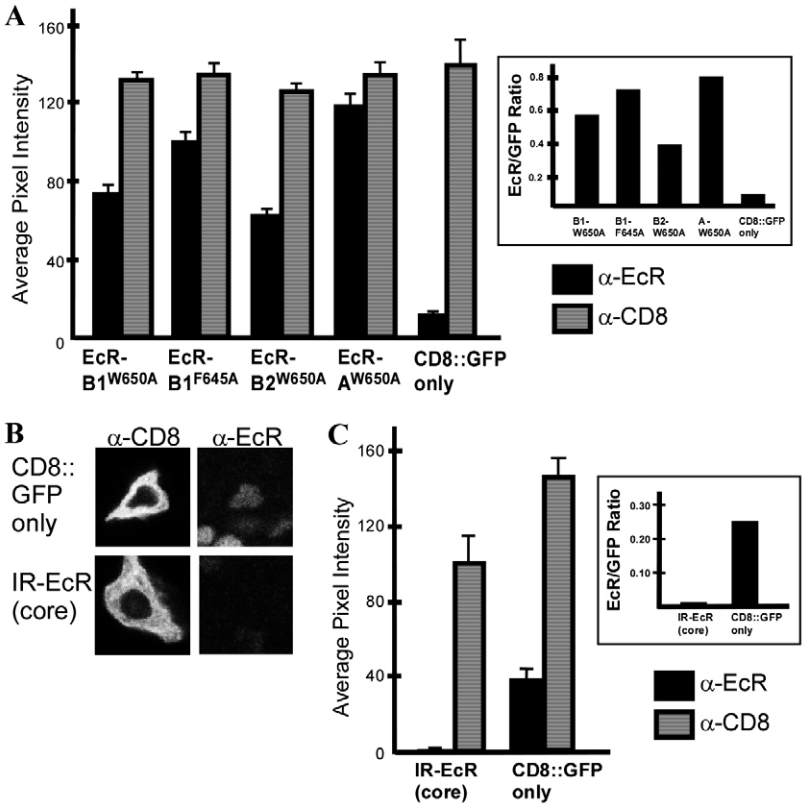

Fig. 7. Quantification of EcR (common) and CD8 immunoreactivity in Tv cell bodies. (**A**) Cells expressing dominant negative, 24 hours apf. Inset shows the EcR to CD8 ratio for each genotype. (**B**) Tv cell bodies, stained with EcR (common) antibody (right) and CD8 antibody (left). (**C**) IR-EcR (core)-expressing cells, late third instar. Inset shows the EcR to CD8 ratio for each.

CD8 immunofluorescence confirmed that the higher levels of EcR in cells expressing EcR-DN was not due to differences in imaging (Fig. 7A, inset). All of the above data support our conclusion that the qualitative differences we see for the different EcR-DNs are not based on quantitative differences in the level of EcR expression.

Effects of IR-EcR (core) on remodeling of the Tv neurons

To further investigate the role of EcR in directing remodeling of the Tv cell axons, we knocked down the level of all EcR isoforms in these cells via an RNAi approach (Roignant et al., 2003). We selectively expressed UAS-IR-EcR (core) and UAS-CD8::GFP in the Tv cells, using the FG10-GAL4 driver. We quantified total EcR protein levels as described above. In the late third instar, Tv cell nuclei from IR-EcR (core) expressing animals showed total EcR levels below the level of detection compared with EcR levels in control animals (Fig. 7B). The ratio of EcR to CD8 protein was much lower for cells containing IR-EcR (core) than those without (Fig. 7C, inset), indicating that the decrease in EcR immunoreactivity was due to a true suppression of EcR protein and not due to immunocytochemistry or imaging artifact. To further insure adequate levels of IR-EcR (core) to knock down EcR level, we raised animals at 29°C until the time of dissection. We compensated for difference in developmental time when comparing IR-EcR (core) data to those from animals maintained at 25°C (Powsner, 1935).

Axonal pruning in the cells expressing IR-EcR (core) resembled the reduced pruning seen in cells expressing the dominant negative EcR constructs. Immunostained nervous systems showed normal larval neurohemal organs at pupariation, but by 24 hours apf, the cells still had larval-like arbors, although they were clearly reduced in size compared with larval stages. We did not see adult-like branches at 24 hours apf (Fig. 8A), but by 48 hours apf and in the adult a new arbor was present that appeared similar to EcR-B1^{F645A}- and EcR-B2^{W650A}-expressing cells. The neurons expressing IR-EcR (core) also had a dense, clumped axon arbor that was surrounded by the reduced adult-like arbor. Comparison of the arbor footprints of cells expressing IR-EcR (core) to control cell arbor footprints emphasizes the decreased branching in these cells (Fig. 8B).

Data from live imaging of cells expressing IR-EcR (core) showed no filopodia during the normal pruning phase (12-18 hours apf) along with a slowed retraction of the larval branches. We first observed filopodia around 24 to 28 hours apf (Fig. 8C). These filopodia formed stable, fasciculated branches, resulting in an adult arbor with both larval and adult characteristics, similar in appearance to arbors of cells expressing EcR-B1^{F645A} and EcR-B2^{W650A}. Fig. 8D shows quantification of filopodial activity of cells expressing IR-EcR (core).

DISCUSSION

Remodeling of Tv neurons

Previous studies on neurite pruning in *Drosophila* at the start of metamorphosis showed the removal of processes by fragmentation (Watts et al., 2003) or a combination of fragmentation and retraction (Williams and Truman, 2005). In both of these cases, surrounding cells participate in the fragmentation process. For the axons of the mushroom body gamma neurons, glial invasion of the axon lobes is necessary for proper pruning (Awasaki and Ito, 2004), whereas for the peripheral dendritic arborizing neurons, phagocytic blood cells are seen to sever proximal and distal regions of the dendritic arbor (Williams and Truman, 2005). In both immunocytochemistry of fixed preparations and time-lapse movies of pruning in the Tv neurons, we saw no sign of fragmentation, even with the addition of hemolymph. In instances where we could visualize individual branches, they were gradually retracted. The fact that Tv axon pruning occurred via retraction only may be partially due to their

peripheral location underneath the basal lamina (Lundquist and Nassel, 1990). This location may isolate them from invading glia within the CNS and phagocytic blood cells circulating in the hemolymph.

Confocal imaging of live Tv cell axons during metamorphosis showed that filopodial activity is a widespread feature of the remodeling neuron. Abundant filopodia were observed during pre-pruning, pruning and outgrowth phases of remodeling. The appearance of filopodia during the pre-pruning period coincides with the time that the Tv cells prune back their dendrites (Schubiger et al., 1998). The axonal structure, however, appears normal at this time, so it is unlikely that these filopodia result from a disruption of the axonal cytoskeleton. The difference in timing between dendrite and axon retraction is also seen in motoneurons MN1-4, which innervate the larval mesothoracic muscles of the larva and remodel to innervate the dorsolongitudinal indirect flight muscles of the adult fly. The dendrites of these neurons undergo retraction between 2 and 4 hours apf, while the axons begin to prune at 6 hours apf and finish at 10 hours apf (Consoulas et al., 2002). In the Tv neurons, filopodia continue to be present as the axonal arbor is retracted. The presence of filopodia during pruning was also observed in the dendritic arborizing neurons (Williams and Truman, 2005). In the mammalian hippocampus, filopodia are associated with both formation and reduction of dendritic spines. Synaptic activation results in growth

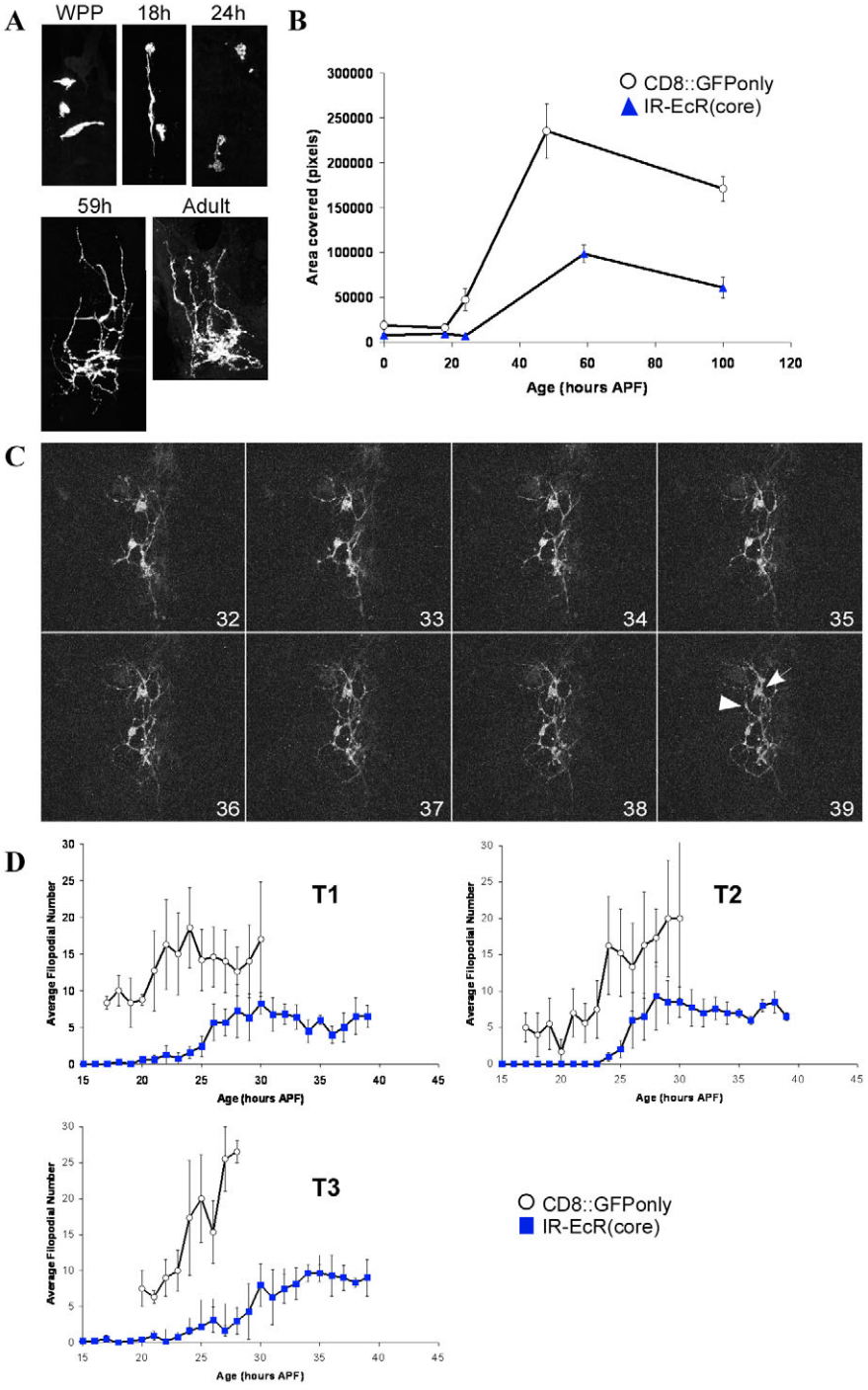

Fig. 8. Expression of IR-EcR (core) in Tv cells during remodeling. (**A**) SCP-labeled, fixed Tv cell axons from cells expressing IR-EcR (core). (**B**) Arbor footprint, from pupariation to adult for control cells and cells expressing IR-EcR (core). (**C**) Live imaging montage of Tv axons (T1, T2 and T3; T1 at top) of UAS-IR-EcR (core)-expressing cells, from 32 to 39 hours apf, 60 minutes apart. Filopodia are present and stabilize into adult-type branches (arrowhead), but the arbor retains a larval-like dense core (arrow). (**D**) Quantification of filopodia on control cells and cells expressing IR-EcR (core).

of dendritic filopodia (Maletic-Savatic et al., 1999), while deafferentation causes filopodial activity followed by reduction of spine density (Benshalom, 1989). It is probable that the presence of filopodia is either a reflection of cytoskeletal instability or plays an active role in disrupting or transporting the cytoskeleton of axons being pruned by retraction.

After pruning is completed, filopodial activity continues as the cell switches to its outgrowth phase. The filopodia present during outgrowth behave differently from earlier filopodia, in that many are precursors to the stable branches that form the adult arbor. Branch stabilization most probably occurs via selective invasion of filopodia by microtubules, as seen in other systems (Sabry et al., 1991; Schaefer et al., 2002). It is unknown if these later filopodia represent a different pharmacological or molecular class from the structures seen during pruning.

Role of ecdysone signaling in pruning

The expression of the EcR dominant negative constructs and the IR-EcR (core) construct in the Tv neurons resulted in incomplete pruning of the larval axonal arbors. Cells expressing any one of these constructs showed a reduction in neurohemal organ size during the pruning period, but substantial larval material was retained into the outgrowth phase. In a study by Williams and Truman (Williams and Truman, 2005) examining pruning in the dendritic arborizing neurons, proximal destabilization of microtubules and thinning of the dendrites was seen before fragmentation. When dominant negative EcR was expressed, the dendrites did not thin proximally. Shortening dendrites with retraction bulbs at their tips were observed, however, indicating that some aspects of pruning still persisted in cells whose steroid-response system was blocked. This indicates that proximal cytoskeletal destabilization may depend on ecdysone signaling in the da neurons, while distal tip retraction may not (Williams and Truman, 2005). One possibility is that distal retraction results from 20E-evoked changes in the epidermis on which the neuron resides. Although fragmentation of Tv cell axons does not occur, the pruning process in these cells may nevertheless be similar to that seen in the da neurons. Destabilization of the cytoskeleton in proximal regions of the axon arbor may facilitate rapid axon retraction. Without activation via ecdysteroid (cells expressing dominant negative EcR or EcR RNAi), cytoskeletal destabilization along the axon shaft may not occur and any pruning must take place via tip retraction with slow retrograde progression. Additionally, cells expressing EcR-DN or IR-EcR (core) lacked filopodia during the pre-pruning and pruning stages. As filopodia are associated with cytoskeletal instability (Benshalom, 1989; Maletic-Savatic et al., 1999), this lack of filopodia may indicate that the cytoskeleton is not destabilizing properly, thereby slowing retraction. Because pruning and early filopodial activity were deficient in cells expressing either the EcR-DNs or IR-EcR (core), we conclude that these events must be mediated by the ecdysteroid activation of transcription (Fig. 9). The fact that the Tv cells prune at all suggests that either the EcR-DNs and the EcR-RNAi are not inactivating the endogenous EcR sufficiently, or that there may also be a non-cell-autonomous component to pruning. As the EcR-DNs are not expressed in the supporting glial cells of the neurohemal organ or in surrounding tissue, these support cells are still responsive to ecdysone. The modified pruning response we see could be due to ecdysone-mediated death of the supporting glial cells or signaling from the surrounding tissue, causing the Tv axons to retract, albeit slowly, as discussed above.

Earlier studies on dendritic pruning of the Tv cells and axonal pruning in the mushroom body showed that the EcR-B isoforms are necessary to support pruning, indicating the need for AF1 activation in this process. That all of the dominant negative EcR isoforms as well as the IR-EcR (core) construct also fail to prune effectively argues that activation through the AF2 domain of EcR is also essential for this process. The EcR-B AF1 and AF2 activation domains probably work cooperatively to bring about the rapid deconstruction of the axonal arbor.

Role of ecdysone signaling in outgrowth

Unlike pruning, outgrowth of Tv cell axons depends on the EcR construct being expressed. Cells expressing EcR-B1^{F645A}, EcR-B2^{W650A} or IR-EcR (core) started to extend filopodia during the outgrowth phase, which began after 24 hours apf. This outgrowth occurred both from filopodia that formed on the remaining larval arbor and from the growth zone underneath. However, new branches that extended from both the larval arbor and the neural outgrowth growth zone were unusual in their morphology. Compared with controls, branches from both sites had small varicosities along their length, resulting in a 'blebby' appearance. In a study by Jacobs and Stevens on cultured PC12 cells, neurites with microtubules depolymerized by Nocodazole showed formation of varicose expansions filled with randomly oriented membranous organelles, by contrast to untreated neurites, in which organelles are uniformly distributed and longitudinally oriented (Jacobs and Stevens, 1986). The Tv neurons in this treatment group may have suffered similar microtubule abnormalities, resulting in formation of similar irregular varicosities.

Cells expressing EcR-B1^{W650A} or EcR-A^{W650A} showed a qualitatively different type of outgrowth, forming very few filopodia and finishing with adult arbors that appeared larval-like and did not

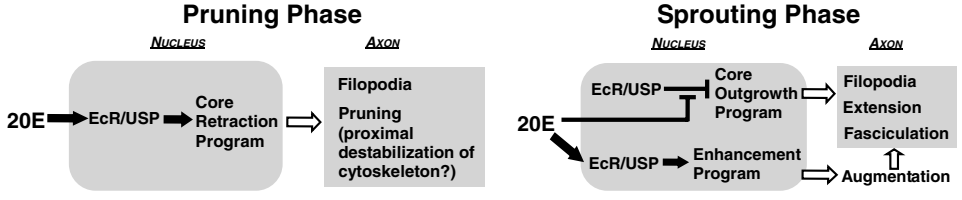

	Filopodia	Pruning
EcR-RNAi	−	−
EcR-B1^{F645A}	−	−
EcR-B2^{W650A}	−	−
EcR-B1^{W650A}	−	−
EcR-A^{W650A}	−	−

	Core Program	Enhancement Program
EcR-RNAi	+	−
EcR-B1^{F645A}	+	−
EcR-B2^{W650A}	+	−
EcR-B1^{W650A}	−	−
EcR-A^{W650A}	−	−

Fig. 9. Conclusions. Model of EcR action and summary of the effects of EcR dominant negative and RNAi treatments during the pruning and sprouting phases of the Tv cell axons.

form a net-like structure over the surface of the nervous system. This draws attention to the importance of filopodia in guiding proper outgrowth to form the adult arbor. Although we observed the extension of rare branches, these seldom sub-branched and did not fasciculate with those from other Tv cells to form the adult-like meshwork. Filopodia actin bundles guide microtubule polymerization in *Aplysia* (Schaefer et al., 2002), while inhibition of F-actin in cultured hamster neurons leads to inhibition of directed growth (Dent and Kalil, 2001; Schaefer et al., 2002). Eradication of filopodia through cytochalasin treatment of grasshopper pioneer neuron growth cones results in disoriented and improper branch formation, but does not eliminate axon extension (Bentley and Toroian-Raymond, 1986). The latter result is similar to our results with the Tv cells, in that growth was not eliminated by lack of filopodia, but instead resulted in a more larval-like arbor in the adult.

EcR dominant negatives, IR-EcR (core) and remodeling

All the constructs produced similar results for pruning, but they had varied effects on outgrowth. These differences in the cellular response to the various EcR constructs indicate that the molecular action of EcR on these neurons may change during the course of their remodeling. The ability of cells expressing IR-EcR (core) to produce filopodia and adult-like branches during the outgrowth period is surprising in the context of 20E acting via activation through the ecdysone receptor. It is possible that the hypomorphic levels of EcR are nevertheless sufficient to support this activation and induce outgrowth. However, similar types of outgrowth were seen in cells expressing EcR-B1^{F645A}, and activation is strongly suppressed by this dominant negative receptor (Cherbas et al., 2003). A more likely hypothesis is that during the outgrowth phase, the ecdysone receptor acts predominantly as a repressor and the role of 20E is to relieve this repression (Fig. 9). The function of the ecdysone receptor as a developmental repressor has been best studied in the developing wing imaginal disc. USP-null clones, which cannot respond to 20E, show precocious sensory neuron differentiation that is no longer dependent on ecdysteroid (Schubiger and Truman, 2000). Expression of IR-EcR (core) in the wing disc similarly leads to precocious neuron development (Schubiger et al., 2005). It is notable that expression of EcR-B1^{F645A} produces a phenotype in the Tv cells that is similar to receptor removal. As this dominant negative can bind 20E (Cherbas et al., 2003), our results suggest that ligand binding by this EcR-DN may relieve the transcriptional repression that it enforces on its target genes, thereby enabling a core program of axonal outgrowth that does not depend on activation. The ability of the EcR-B1^{F645A} dominant negative to support derepression, however, may be highly context-dependent, as there were no differences seen in activation or inhibition in Kc167 cells expressing either EcR-B1^{F645A} or EcR-B1^{W650A} (Hu et al., 2003).

This hypothesis, that the ecdysone receptor plays a permissive role as a repressor during the phase of neuronal outgrowth during remodeling, is reinforced by the results from cells expressing EcR-A^{W650A} and EcR-B1^{W650A}, because these cells show a more severe phenotype than that seen in cells with knocked-down EcR levels (Figs 5 and 8). However, the phenotype of cells expressing EcR-B2^{W650A} was less severe in both immunocytochemistry and live imaging than those expressing EcR-A^{W650A} and EcR-B1^{W650A}. Experiments testing the activation potential of each of the wild-type EcR isoforms indicated the presence of a repression domain in the A/B region of EcR-A (Mouillet et al., 2001). Only an activation domain (AF1) has been ascribed to the A/B region of EcR-B1 (Hu et al., 2003; Mouillet et al., 2001), but this region is relatively long and incompletely characterized. We suggest that the A/B region of EcR-B1 may also possess a repression domain, although this needs to be confirmed biochemically. If this were the case, then either of these isoforms would then be able to tether a strong co-repressor complex that could not be removed without ecdysteroid binding. Under this hypothesis, the weak phenotype seen with expression of the EcR-B2^{W650A} construct may be a function of its short A/B region. This isoform has a strong AF1 activational function in its 17 amino acid A/B region, but it is unlikely that this short region also contains a repressive domain. Because of this, the EcR-B2 isoform may not be able to assemble the strong co-repressor complexes that are seen with the other isoforms. Hence, the EcR-B2 isoform may be able to mediate strong activation but be a very poor repressor. This model would account for the fact that in axon outgrowth, a situation where the crucial step is the relief of transcriptional repression by ecdysteroid binding to its receptor, cells expressing EcR-A^{W650A} or EcR-B1^{W650A} have a much more severe phenotype than cells expressing EcR-B2^{W650A}, EcR-B1^{F645A} or IR-EcR (core).

These studies indicate that EcR function is complex, with expression of isoforms and co-factors, hormone titer, and derepression versus activation of target genes varying through space and time. However, studies of the effects of EcR on neuronal remodeling in combination with new technology are yielding invaluable information on the role of nuclear receptors in the development of the nervous system.

We thank C. Antoniewski for supplying the UAS-IR-EcR (core) fly strain, S. Robinow for supplying the FG10-Gal4 fly strain, Nancy Thompson for injection of fly embryos and Eric VanHaaften for assistance in plasmid construction. The antibody SCP was provided by D. Willows, and the antibody IID 9.6 was provided by W. Talbot and D. Hogness. Helpful comments on the manuscript were received from an anonymous reviewer. Research was supported by NIH grants NS 13079 and NS 29971 to J.W.T. and NSF award MCB-0077841 to P.C. H.B. was supported by NIH Training Grant 5T32 HD07183.

References

Awasaki, T. and Ito, K. (2004). Engulfing action of glial cells is required for programmed axon pruning during Drosophila metamorphosis. *Curr. Biol.* **14**, 668-677.

Bai, J., Uehara, Y. and Montell, D. J. (2000). Regulation of invasive cell behavior by taiman, a Drosophila protein related to AIB1, a steroid receptor coactivator amplified in breast cancer. *Cell* **103**, 1047-1058.

Benshalom, G. (1989). Structural alterations of dendritic spines induced by neural degeneration of their presynaptic afferents. *Synapse* **4**, 210-222.

Bentley, D. and Toroian-Raymond, A. (1986). Disoriented pathfinding by pioneer neurone growth cones deprived of filopodia by cytochalasin treatment. *Nature* **323**, 712-715.

Brand, A. H. and Perrimon, N. (1993). Targeted gene expression as a means of altering cell fates and generating dominant phenotypes. *Development* **118**, 401-415.

Cherbas, L., Lee, K. and Cherbas, P. (1991). Identification of ecdysone response elements by analysis of the Drosophila Eip28/29 gene. *Genes Dev.* **5**, 120-131.

Cherbas, L., Hu, X., Zhimulev, I., Belyaeva, E. and Cherbas, P. (2003). EcR isoforms in Drosophila: testing tissue-specific requirements by targeted blockade and rescue. *Development* **130**, 271-284.

Consoulas, C., Restifo, L. L. and Levine, R. B. (2002). Dendritic remodeling and growth of motoneurons during metamorphosis of Drosophila melanogaster. *J. Neurosci.* **22**, 4906-4917.

Dela Cruz, F. E., Kirsch, D. R. and Heinrich, J. N. (2000). Transcriptional activity of Drosophila melanogaster ecdysone receptor isoforms and ultraspiracle in Saccharomyces cerevisiae. *J. Mol. Endocrinol.* **24**, 183-191.

Dent, E. W. and Kalil, K. (2001). Axon branching requires interactions between dynamic microtubules and actin filaments. *J. Neurosci.* **21**, 9757-9769.

Dressel, U., Thormeyer, D., Altincicek, B., Paululat, A., Eggert, M., Schneider, S., Tenbaum, S. P., Renkawitz, R. and Baniahmad, A. (1999). Alien, a highly conserved protein with characteristics of a corepressor for members of the nuclear hormone receptor superfamily. *Mol. Cell. Biol.* **19**, 3383-3394.

Gibbs, S. M. and Truman, J. W. (1998). Nitric oxide and cyclic GMP regulate retinal patterning in the optic lobe of Drosophila. *Neuron* **20**, 83-93.

Hu, X., Cherbas, L. and Cherbas, P. (2003). Transcription activation by the

ecdysone receptor (EcR/USP): identification of activation functions. *Mol. Endocrinol.* **17**, 716-731.
Jacobs, J. R. and Stevens, J. K. (1986). Experimental modification of PC12 neurite shape with the microtubule-depolymerizing drug Nocodazole: a serial electron microscopic study of neurite shape control. *J. Cell Biol.* **103**, 907-915.
Kiehart, D. P., Montague, R. A., Rickoll, W. L., Foard, D. and Thomas, G. H. (1994). High-resolution microscopic methods for the analysis of cellular movements in Drosophila embryos. *Methods Cell Biol.* **44**, 507-532.
Koelle, M. R., Talbot, W. S., Segraves, W. A., Bender, M. T., Cherbas, P. and Hogness, D. S. (1991). The Drosophila EcR gene encodes an ecdysone receptor, a new member of the steroid receptor superfamily. *Cell* **67**, 59-77.
Kozlova, T. and Thummel, C. S. (2000). Steroid regulation of postembryonic development and reproduction in Drosophila. *Trends Endocrinol. Metab.* **11**, 276-280.
Lee, T. and Luo, L. (1999). Mosaic analysis with a repressible cell marker for studies of gene function in neuronal morphogenesis. *Neuron* **22**, 451-461.
Lee, T., Marticke, S., Sung, C., Robinow, S. and Luo, L. (2000). Cell-autonomous requirement of the USP/EcR-B ecdysone receptor for mushroom body neuronal remodeling in Drosophila. *Neuron* **28**, 807-818.
Lundquist, T. and Nassel, D. R. (1990). Substance P-, FMRFamide-, and gastrin/cholecystokinin-like immunoreactive neurons in the thoraco-abdominal ganglia of the flies Drosophila and Calliphora. *J. Comp. Neurol.* **294**, 161-178.
Maletic-Savatic, M., Malinow, R. and Svoboda, K. (1999). Rapid dendritic morphogenesis in CA1 hippocampal dendrites induced by synaptic activity. *Science* **283**, 1923-1927.
Masinovsky, B., Kempf, S. C., Callaway, J. C. and Willows, A. O. (1988). Monoclonal antibodies to the molluscan small cardioactive peptide SCPB: immunolabeling of neurons in diverse invertebrates. *J. Comp. Neurol.* **273**, 500-512.
Mouillet, J. F., Henrich, V. C., Lezzi, M. and Vogtli, M. (2001). Differential control of gene activity by isoforms A, B1 and B2 of the Drosophila ecdysone receptor. *Eur. J. Biochem.* **268**, 1811-1819.
Nassel, D. R., Holmqvist, M. H., Hardie, R. C., Hakanson, R. and Sundler, F. (1988). Histamine-like immunoreactivity in photoreceptors of the compound eyes and ocelli of the flies Calliphora erythrocephala and Musca domestica. *Cell Tissue Res.* **253**, 639-646.
Powsner, L. (1935). The effects of temperature on duration of developmental stages of Drosophila melanogaster. *Physiol. Zool.* **8**, 474-520.
Robinson-Rechavi, M., Escriva Garcia, H. and Laudet, V. (2003). The nuclear receptor superfamily. *J. Cell Sci.* **116**, 585-586.
Roignant, J. Y., Carre, C., Mugat, B., Szymczak, D., Lepesant, J. A. and Antoniewski, C. (2003). Absence of transitive and systemic pathways allows cell-specific and isoform-specific RNAi in Drosophila. *Rna* **9**, 299-308.
Sabry, J. H., O'Connor, T. P., Evans, L., Toroian-Raymond, A., Kirschner, M. and Bentley, D. (1991). Microtubule behavior during guidance of pioneer neuron growth cones in situ. *J. Cell Biol.* **115**, 381-395.
Schaefer, A. W., Kabir, N. and Forscher, P. (2002). Filopodia and actin arcs guide the assembly and transport of two populations of microtubules with unique dynamic parameters in neuronal growth cones. *J. Cell Biol.* **158**, 139-152.
Schubiger, M. and Truman, J. W. (2000). The RXR ortholog USP suppresses early metamorphic processes in Drosophila in the absence of ecdysteroids. *Development* **127**, 1151-1159.
Schubiger, M., Wade, A. A., Carney, G. E., Truman, J. W. and Bender, M. (1998). Drosophila EcR-B ecdysone receptor isoforms are required for larval molting and for neuron remodeling during metamorphosis. *Development* **125**, 2053-2062.
Schubiger, M., Tomita, S., Sung, C., Robinow, S. and Truman, J. W. (2003). Isoform specific control of gene activity in vivo by the Drosophila ecdysone receptor. *Mech. Dev.* **120**, 909-918.
Schubiger, M., Carre, C., Antoniewski, C. and Truman, J. W. (2005). Ligand-dependent de-repression via EcR/USP acts as a gate to coordiate the differentiation of sensory neurons in the Drosophila wing. *Development* **132**, 5239-5248.
Sedkov, Y., Cho, E., Petruk, S., Cherbas, L., Smith, S. T., Jones, R. S., Cherbas, P., Canaani, E., Jaynes, J. B. and Mazo, A. (2003). Methylation at lysine 4 of histone H3 in ecdysone-dependent development of Drosophila. *Nature* **426**, 78-83.
Suster, M. L., Martin, J. R., Sung, C. and Robinow, S. (2003). Targeted expression of tetanus toxin reveals sets of neurons involved in larval locomotion in Drosophila. *J. Neurobiol.* **55**, 233-246.
Talbot, W. S., Swyryd, E. A. and Hogness, D. S. (1993). Drosophila tissues with different metamorphic responses to ecdysone express different ecdysone receptor isoforms. *Cell* **73**, 1323-1337.
Tissot, M. and Stocker, R. F. (2000). Metamorphosis in drosophila and other insects: the fate of neurons throughout the stages. *Prog. Neurobiol.* **62**, 89-111.
Truman, J. (2005). Hormonal control of the form and function of the nervous system. In *Comprehensive Molecular Insect Science*. Vol. 2 (ed. L. I. Gilbert, K. Iatrou and S. S. Gill), pp. 135-163. Amsterdam: Elsevier.
Truman, J. W., Talbot, W. S., Fahrbach, S. E. and Hogness, D. S. (1994). Ecdysone receptor expression in the CNS correlates with stage-specific responses to ecdysteroids during Drosophila and Manduca development. *Development* **120**, 219-234.
Tsai, C. C., Kao, H. Y., Yao, T. P., McKeown, M. and Evans, R. M. (1999). SMRTER, a Drosophila nuclear receptor coregulator, reveals that EcR-mediated repression is critical for development. *Mol. Cell* **4**, 175-186.
Watts, R. J., Hoopfer, E. D. and Luo, L. (2003). Axon pruning during Drosophila metamorphosis: evidence for local degeneration and requirement of the ubiquitin-proteasome system. *Neuron* **38**, 871-885.
Weeks, J. C. (1999). Steroid hormones, dendritic remodeling and neuronal death: insights from insect metamorphosis. *Brain Behav. Evol.* **54**, 51-60.
Weeks, J. C. and Truman, J. W. (1985). Independent steroid control of the fates of motoneurons and their muscles during insect metamorphosis. *J. Neurosci.* **5**, 2290-2300.
Williams, D. W. and Truman, J. W. (2005). Cellular mechanisms of dendrite pruning in Drosophila: insights from in vivo time-lapse of remodeling dendritic arborizing sensory neurons. *Development* **132**, 3631-3642.
Yao, T. P., Segraves, W. A., Oro, A. E., McKeown, M. and Evans, R. M. (1992). Drosophila ultraspiracle modulates ecdysone receptor function via heterodimer formation. *Cell* **71**, 63-72.